Emergence of decoherence by incoherent manifestation of coherent quantum fluctuations

2009 J. Phys. A: Math. Theor. 42 145302

(http://iopscience.iop.org/1751-8121/42/14/145302)

IOP PUBLISHING JOURNAL OF PHYSICS A: MATHEMATICAL AND THEORETICAL

J. Phys. A: Math. Theor. **42** (2009) 145302 (20pp) doi:10.1088/1751-8113/42/14/145302

Emergence of decoherence by incoherent manifestation of coherent quantum fluctuations

Murat Çetinbaş

Laboratory for Advanced Spectroscopy and Imaging Research, 4D LABS and Department of Chemistry, Simon Fraser University, Burnaby, BC, V5A 1S6, Canada

E-mail: cetinbas@sfu.ca

Received 7 October 2008, in final form 9 January 2009
Published 16 March 2009
Online at stacks.iop.org/JPhysA/42/145302

Abstract

The interaction of a quantum system with its surrounding environment results in losses of quantum correlations in the state of the system due to a decoherence process. The origin of decoherence is often attributed to the system–environment entanglement, which is not the only source of decoherence, however. Here we show that environment-induced coherent quantum fluctuations, i.e. Lamb or Stark shift-like effects, can also lead to the emergence of decoherence, which we call an incoherence process, even in the absence of the system–environment entanglement. We isolate the incoherence process from a general decoherence dynamics and formulate the exact equation of motion governing the incoherence dynamics in the absence of entanglement-induced decoherence. We exemplify the incoherence dynamics for a number of different situations including chaotic, regular and decoherence-free environments.

PACS numbers: 03.65.−w, 05.30.−d, 03.65.Yz, 03.67.Lx

(Some figures in this article are in colour only in the electronic version)

1. Introduction

Entanglement and decoherence are two distinguishing features of quantum mechanics with no classical analog. Entanglement is a key ingredient of quantum information theory [1], with applications ranging from quantum teleportation [2], quantum key distribution [3], super dense coding [4] to telecloning [5]. While entanglement is rightfully a desirable feature, the entanglement of a quantum system with its surrounding environment also leads to decoherence [6, 7], which is one of the primary obstacles on the roadway to the development of quantum information technologies [1]. Understanding the underlying mechanisms behind these two phenomena and especially the interplay between them is of fundamental importance and is the subject of numerous studies [1–15].

In the course of open system dynamics [6–15], a quantum subsystem loses its well-defined quantum correlations due to interactions with its surrounding environment. This process, by and large, is known as decoherence. The system–environment entanglement (SEE) is one of the well-known, but not the only, sources of decoherence. Hence, decoherence may not be avoided even in the absence of SEE. The subject matter of this paper is an alternative mechanism of decoherence, which induces irreversibility (i.e. non-unitarity) into quantum dynamics even if a quantum subsystem of interest is not entangled with its surrounding environment. Henceforth, we refer to the decoherence phenomenon in question, which emanates from environment-induced coherent quantum fluctuations, as *incoherence*, whereas we refer to the decoherence, which manifests due to the SEE, as *entanglement-induced decoherence* (EID).

In a general decoherence scenario, in which a quantum subsystem might be subject to EID as well as incoherence, one may not be able to distinguish between these two processes. This is because both processes induce irreversibility into quantum dynamics and cause the subsystem's state to lose its purity. However, the mechanism of irreversibility induced by these two processes is of a different physical origin. To establish the differences, one can imagine a quantum subsystem interacting with an equilibrium environment, the state of which is of non-zero entropy represented by a Gibbs state. EID occurs due to the entanglement of the subsystem's state with possibly each pure state component of the Gibbs state. Hence, EID is a correlation transfer process between the states of the subsystem and its surrounding environment. Incoherence does not necessitate the SEE, but it should be expected whenever an open quantum system is subject to environment-induced coherent shifting. Effects of this kind are also known as Lamb or Stark shift-like effects in the theory of open system dynamics [8]. In the presence of coherent shifting, the subsystem Hamiltonian is shifted in a slightly different magnitude for each pure state component of the Gibbs state. As a result, the subsystem experiences coherent quantum fluctuations. During the incoherence process, quantum correlations of the subsystem do not leak into the environment; nevertheless, the state of the subsystem becomes a statistical mixture due to an incoherent superposition of coherent probability amplitudes. Hence, the incoherence, in essence, is a non-unitary manifestation of unitary quantum fluctuations.

In this study, we completely detach the incoherence process from a general decoherence dynamics and deliver an exact formulation of *absolute* incoherence dynamics, namely incoherence dynamics in the absence of EID. While incoherence is an intrinsic feature of open system dynamics, to our knowledge, no attempt has been made for an exact formulation of absolute incoherence dynamics, which is quite straightforward, once certain conditions annulling the SEE are determined. We establish a certain symmetry condition on system–environment interactions to avoid the SEE, and by starting from first principles and with quite general assumptions, we formulate the exact equation of motion for an arbitrary quantum system (interacting with an arbitrary environment) undergoing the absolute incoherence process. Hereafter, unless otherwise stated for emphasis, we refer to the absolute incoherence simply as incoherence.

The exact formulation of the incoherence dynamics, without any restriction on system or environment Hamiltonians, requires a certain symmetry condition on interaction Hamiltonians so that the SEE can be avoided. To determine this symmetry condition, we utilize the theory of decoherence-free subspaces (DFSs) [16–19]. We show that the SEE can be avoided when an environment evolves in a DFS. While the dynamics of the environment evolves unitarily in a DFS, it turns out that the subsystem dynamics is non-unitary. By using the decoherence-free environment (DFE) condition, we derive an exact Kraus decomposition [12] for the subsystem density in which each Kraus operator in the decomposition takes an explicit form. The

resulting Kraus decomposition defines the exact equation of motion for incoherence dynamics in the absence of EID.

We borrow the term 'incoherence' from nuclear magnetic resonance (NMR) quantum computation studies [20]. The mechanism of incoherence studied here is reminiscent of the mechanism of incoherence or dephasing of spins in NMR studies [20]. In a typical NMR experiment, the spins of an ensemble experience the external field in slightly different magnitudes. While each spin of the ensemble evolves unitarily, the dynamics of the ensemble appears to be non-unitary. Hence, the incoherence in NMR studies [20] is defined as a loss of purity in the ensemble-averaged state while the decoherence refers to a loss of purity in the states of individual spins. Here our interest is not in an ensemble, but in an individual quantum system. In the context of NMR, our focus is then on the incoherence process in the decoherence dynamics of an individual spin. Hence, the incoherence process formulated here is a component of decoherence dynamics and therefore should be distinguished from the incoherence phenomenon in NMR studies [20].

Incoherence dynamics may appear in certain master equations [21], in an exactly solvable spin-bath model [22] or in the semi-classical limit, where the SEE may be negligible; a quantum system interacting with a chaotic bath of thermodynamic dimension undergoes only incoherence dynamics [23]. In principle, any condition nullifying the SEE should suffice the emergence of absolute incoherence dynamics. Interesting cases arise for non-standard models of decoherence. For example, it has been shown that chaotic intra-environmental interactions suppress EID [23–28]. More recently, we have also shown that fast environmental dynamics leads to a rapid suppression of EID [29]. In such cases, EID can be suppressed and the incoherence process emerges as the only source of decoherence. Here, by comparison between exact numerical and Kraus decomposition calculations, we demonstrate the onset of absolute incoherence as a result of suppression of EID for a number of different situations including chaotic, regular and DFEs by studying the open dynamics of a qubit in an isolated quantum computer (QC) core with static internal imperfections [30].

The organization of this paper is as follows. In section 2, we drive the exact quantum equation of motion for incoherence dynamics. In section 3, we present our spin spin–bath model. In section 4, we report our results. In section 5, we discuss these results. In section 6, we conclude our study.

2. Formulation of incoherence dynamics

Starting from first principles, we aim at formulating incoherence dynamics for an arbitrary quantum subsystem interacting with an arbitrary environment. In this section, we first outline the operator sum representation of the open system dynamics [12]. Second, we review the Hamiltonian formulations of DFSs [16–19] and determine the required conditions under which an environment evolves in a DFS. Third, by using the fact that the SEE is avoided under the DFE condition we obtain an exact Kraus decomposition governing incoherence dynamics.

2.1. Operator sum representation

We consider a quantum subsystem of interest and its surrounding environment as a bipartite closed system represented by a total Hamiltonian of the form

$$\hat{H} = \hat{H}_S + \sum_{\mu} \hat{S}_\mu \hat{B}_\mu + \hat{H}_B, \tag{1}$$

where $\hat{H}_S$ is the subsystem, $\hat{S}_\mu \hat{B}_\mu$ are the interactions and $\hat{H}_B$ is the environment or bath Hamiltonians. The exact quantum dynamics evolves unitarily from the Liouville–von Neumann equation, the solution of which is of the form

$$\hat{\rho}(t) = \hat{U}(t)\hat{\rho}(0)\hat{U}^\dagger(t), \tag{2}$$

where $\hat{U}(t) = \exp\{-(\mathrm{i}/\hbar)\hat{H}t\}$ is the unitary operator governing the dynamics and $\hat{\rho}(0) = \hat{\rho}_S(0) \otimes \hat{\rho}_B(0)$ is the total initial density operator of a product form for the system and bath degrees of freedom. While we leave the initial system density $\hat{\rho}_S(0)$ unspecified, we assume that the bath density is diagonal in the energy basis $\hat{\rho}_B(0) = \sum_m p_m |m\rangle\langle m|$, where $\hat{H}_B|m\rangle = E_m|m\rangle$, and the usual completeness relations are $\sum_m |m\rangle\langle m| = \hat{I}_B$ and $\langle n|m\rangle = \delta_{n,m}$. Due to thermodynamics considerations, an appropriate choice of a bath state is of a canonical form for which bath populations are given by $p_m = \exp\{-\beta E_m\} \big/ \sum_n \exp\{-\beta E_n\}$ for a fixed inverse temperature $\beta = 1/k_B T$, where k_B is the Boltzmann constant.

To obtain the time-evolved subsystem density $\hat{\rho}_S(t)$, we trace over the bath degree of freedom, $\hat{\rho}_S(t) = \mathrm{Tr}_B\{\hat{U}(t)\hat{\rho}(0)\hat{U}^\dagger(t)\}$, by using the complete bath eigenbasis $\{|n\rangle\}$,

$$\hat{\rho}_S(t) = \sum_{n,m} p_m \langle n|\hat{U}(t)|m\rangle \hat{\rho}_S(0) \langle m|\hat{U}^\dagger(t)|n\rangle, \tag{3}$$

which can be written in the following compact form:

$$\hat{\rho}_S(t) = \sum_{n,m} \hat{\mathcal{K}}_{n,m}(t)\hat{\rho}_S(0)\hat{\mathcal{K}}^\dagger_{n,m}(t), \tag{4}$$

in terms of the Kraus operators

$$\hat{\mathcal{K}}_{n,m}(t) = \sqrt{p_m}\langle n|\hat{U}(t)|m\rangle. \tag{5}$$

The Kraus decomposition (4) describes a general decoherence scenario in which a quantum subsystem evolves under the influences of both EID and incoherence processes. These processes can be distinguished by rewriting (4) in the form

$$\hat{\rho}_S(t) = \sum_n \hat{\mathcal{K}}_{n,n}(t)\hat{\rho}_S(0)\hat{\mathcal{K}}^\dagger_{n,n}(t) + \sum_{n,m} \hat{\mathcal{K}}_{n,m}(t)\hat{\rho}_S(0)\hat{\mathcal{K}}^\dagger_{n,m}(t)\delta^{-1}_{n,m}, \tag{6}$$

where $\delta^{-1}_{n,m} = 1$ for $n \neq m$ and $\delta^{-1}_{n,m} = 0$ for $n = m$. We will show that the second sum above, responsible for EID, vanishes when the interaction Hamiltonians cannot generate the SEE and the first sum induces the incoherence process.

2.2. Decoherence-free environments

In this section, by exploiting certain symmetry conditions on the system–environment interactions we eliminate the SEE. To do so, we refer to the theory of DFSs [16–19]. In the following, we briefly review the basic ideas behind the Hamiltonian formulations of DFSs [16–19] and determine conditions for DFEs.

A DFS is a subspace in which the quantum dynamics is unitary even in the presence of system–environment interactions. To construct a DFS, one starts with the assumption [16] that there exists a set of degenerate eigenvectors of system coupling operators such that $\hat{S}_\mu|\tilde{s}\rangle = s_\mu|\tilde{s}\rangle$. Accordingly, if $\hat{H}_S$ leaves the subspace $\tilde{\mathcal{H}}_S$, spanned by these eigenvectors $\tilde{\mathcal{H}}_S = \mathrm{span}\{|\tilde{s}\rangle\}$ invariant, it follows that the dynamics initiated within a DFS evolves unitarily in this DFS [16–18]. Determining a similar condition for a DFE is effortless. Trivially, one only needs to interchange the roles of system and environment. Hence, by stipulating

that the degenerate eigenvectors $\hat{B}_\mu|\tilde{b}\rangle = b_\mu|\tilde{b}\rangle$ exist and span the DFS for the environment $\tilde{\mathcal{H}}_B = \text{span}\{|\tilde{b}\rangle\}$, the total Hamiltonian in the basis $\{|\tilde{b}\rangle\}$ can be expressed as

$$\hat{H} = \left[\hat{H}_S + \sum_\mu \hat{S}_\mu b_\mu\right] \otimes \hat{I}_B + \hat{1}_S \otimes \hat{H}_B = \tilde{H}_S \otimes \hat{I}_B + \hat{1}_S \otimes \hat{H}_B, \tag{7}$$

which clearly enables us to decouple the system and bath dynamics:

$$\hat{\rho}(t) = \tilde{U}_S(t)\hat{\rho}_S(0)\tilde{U}_S^\dagger(t) \otimes \hat{U}_B(t)\hat{\rho}_B(0)\hat{U}_B^\dagger(t), \tag{8}$$

where $\tilde{U}_S(t) = \exp\{-(\mathrm{i}/\hbar)\tilde{H}_S t\}$ and $\hat{U}_B(t) = \exp\{-(\mathrm{i}/\hbar)\hat{H}_B t\}$. Note that since the system and bath dynamics are decoupled, the time evolution cannot generate the SEE. By tracing $\hat{\rho}(t)$ over the system degree of freedom, one can readily show that the environment evolves in a decoherence-free fashion, i.e.

$$\hat{\rho}_B(t) = \text{Tr}_S\{\hat{\rho}(t)\} = \hat{U}_B(t)\hat{\rho}_B(0)\hat{U}_B^\dagger(t). \tag{9}$$

However, since an environment in many situations is the uncontrollable degree of freedom, finding the appropriate *degenerate* basis $\{|\tilde{b}\rangle\}$ for a DFE is a rather mysterious task, if at all possible. In this regard, our choice of the appropriate basis is somewhat limited, yet this limitation leads us to a rather obvious choice of basis. Due to thermodynamic considerations, we have already assumed that the bath density $\hat{\rho}_B(0)$ is diagonal in the energy representation. Hence, $\hat{\rho}_B(0)$ is a function of the bath Hamiltonian $\hat{H}_B$ so that $[\hat{\rho}_B(0), \hat{H}_B] = 0$. In what follows, we demand that the bath coupling operators commute with the bath Hamiltonian, i.e. $[\hat{B}_\mu, \hat{H}_B] = 0$. Hence, our DFE condition is that the family of operators $\mathfrak{F} \equiv \{\hat{B}_\mu, \hat{H}_B\}$ consists of mutually commuting Hermitian operators and therefore $\mathfrak{F}$ is simultaneously diagonalizable.

Let the eigenbasis $\{|n\rangle\}$ denote the complete set of eigenfunctions diagonalizing $\hat{H}_B$, i.e. $\hat{H}_B|n\rangle = E_n|n\rangle$ and thus $\hat{B}_\mu|n\rangle = b_\mu^n|n\rangle$. The total Hamiltonian in this basis $\{|n\rangle\}$ has the representation

$$\hat{H} = \hat{H}_S \otimes \hat{1}_B + \sum_\mu \hat{S}_\mu \otimes \sum_n b_\mu^n|n\rangle\langle n| + \hat{1}_S \otimes \sum_n E_n|n\rangle\langle n|. \tag{10}$$

Defining the initial states of the form $\hat{\rho}_n(0) = \hat{\rho}_S(0)\otimes|n\rangle\langle n|$, the solution of the Liouville–von Neumann equation (2) can be written as

$$\hat{\rho}(t) = \sum_n p_n\hat{\rho}_n(t) \qquad \text{and} \qquad \hat{\rho}_n(t) = \hat{U}(t)\hat{\rho}_n(0)\hat{U}^\dagger(t). \tag{11}$$

The form of the total Hamiltonian (10) suggests that the action of the propagator $\hat{U}(t)$ on each $\hat{\rho}_n(0)$ is as follows:

$$\hat{\rho}_n(t) = \hat{U}_S^n(t)\hat{\rho}_S(0)\hat{U}_S^{n\dagger}(t) \otimes \hat{U}_B(t)|n\rangle\langle n|\hat{U}_B^\dagger(t). \tag{12}$$

Here $\hat{U}_S^n(t) = \exp\{-(\mathrm{i}/\hbar)\hat{H}_S^n t\}$, where $\hat{H}_S^n = \hat{H}_S + \sum_\mu \hat{S}_\mu b_\mu^n$. It is clear from equation (12) that the time evolution cannot generate the SEE. In what follows, since $\text{Tr}_S\{\hat{U}_S^n(t)\hat{\rho}_S(0)\hat{U}_S^{n\dagger}(t)\} = 1$ for each n, by tracing $\hat{\rho}(t)$ over the system degree of freedom, we obtain the DFE evolution

$$\hat{\rho}_B(t) = \text{Tr}_S\{\hat{\rho}(t)\} = \hat{U}_B(t)\hat{\rho}_B(0)\hat{U}_B^\dagger(t). \tag{13}$$

It is noteworthy that the latter definition of DFEs is different than the former definition in terms of simultaneous degenerate eigenstates. The latter definition is equivalent to the original definition of DFSs by Zurek [19] in terms of pointer states, which does not require the degeneracy of eigenstates. While both definitions lead to DFEs, as we point out in the following section, they do have fundamentally different consequences on the subsystem dynamics.

2.3. Kraus decomposition of incoherence process

In the previous section, our focus was on the environment degree of freedom, and we have shown that the SEE cannot be generated under the DFE conditions. In this section, we focus on the subsystem degree of freedom and explore open system dynamics under the DFE conditions.

For each time-evolved state $\hat{\rho}_n(t)$, tracing equation (12) over the environment degree of freedom gives

$$\mathrm{Tr}_B\{\hat{\rho}_n(t)\} = \hat{U}_S^n(t)\hat{\rho}_S(0)\hat{U}_S^{n\dagger}(t), \tag{14}$$

by using which, the time evolution of the subsystem density can now be expressed as

$$\hat{\rho}_S(t) = \sum_n \hat{\mathcal{K}}_{n,n}(t)\hat{\rho}_S(0)\hat{\mathcal{K}}_{n,n}^{\dagger}(t) \tag{15}$$

in terms of the Kraus operators

$$\hat{\mathcal{K}}_{n,n}(t) = \sqrt{p_n}\exp\left\{-(\mathrm{i}/\hbar)\left(\hat{H}_S + \sum_\mu \hat{S}_\mu b_\mu^n\right)t\right\}. \tag{16}$$

Equation (15) is the final form of the Kraus decomposition, which defines the exact equation of motion for a subsystem density undergoing incoherence dynamics in the absence of SEE.

The irreversibility brought about by the Kraus decomposition (15) emerges from the environment-induced coherent shifting. Each pure state component of the thermal bath state shifts the free system Hamiltonian as $\hat{H}_S \to \hat{H}_S^n = \hat{H}_S + \sum_\mu \hat{S}_\mu b_\mu^n$. Presuming that $b_\mu^n \neq b_\mu^m$, i.e. the diagonal matrix elements of $\hat{B}_\mu$ are all different, the state of the subsystem evolves under M slightly different shifted-system Hamiltonians, where M refers to the number of populated bath states for a given bath temperature. Each shifted-system Hamiltonian changes the coherent probability amplitude of a subsystem's state by a slightly different magnitude. The convex combination of these probability amplitudes results in destructive interferences which in turn induce the non-unitary dynamics.

The normalization condition for the Kraus operators $\sum_n \hat{\mathcal{K}}_{n,n}(t)\hat{\mathcal{K}}_{n,n}^{\dagger}(t) = \hat{I}_S$ indicates that the open system dynamics is unitary, provided that the Kraus decomposition (15) has only one term or one type of terms. Hence, a pure environment state does not induce irreversibility into the subsystem dynamics, which means that while the coherent shift process does not cease, the incoherence can be suppressed at absolute zero temperature. However, there is no such restriction on the EID which manifests as long as the system and environment states are entangled even at absolute zero temperature. The incoherence dynamics is also unitary when $b_\mu^n = b_\mu$, i.e. the bath coupling operators are the scalar operators $\hat{B}_\mu = b_\mu \hat{I}_B$. In such cases, the Kraus decomposition includes only one type of terms and is reduced to the form

$$\hat{\rho}_S(t) = \hat{\mathcal{K}}(t)\hat{\rho}_S(0)\hat{\mathcal{K}}^{\dagger}(t), \qquad \text{where} \quad \hat{\mathcal{K}}(t) = \exp\left\{-(\mathrm{i}/\hbar)\left(\hat{H}_S + \sum_\mu \hat{S}_\mu b_\mu\right)t\right\}. \tag{17}$$

Hence, the open system dynamics is unitary but is also shifted. Note that the above form of Kraus decomposition can be achieved for the DFS condition $\hat{B}_\mu|\tilde{b}\rangle = b_\mu|\tilde{b}\rangle$. Indeed, by tracing equation (8) over the environment degree of freedom one can obtain the decoherence-free evolution given by equation (17). Thus, the existence of degenerate eigenstates leads to decoherence-free time evolutions for both the system and environment.

Interestingly, the equation of motion (15) of incoherence dynamics is identical to the chaotic Kraus decomposition (CKD) derived in our previous studies [23]. Hence, the CKD only predicts incoherence dynamics but nothing more. The derivation of the CKD is based

on the fact that the square of the off-diagonal matrix elements of the bath coupling operators vanishes in the eigenbasis of a large chaotic bath Hamiltonian, i.e. $|\langle n|\hat{B}_\mu|m\rangle|^2 \to 0$ when $N \to \infty$, where N is the number of bath modes. In previous studies of the CKD [23], the incoherence phenomenon is not appreciated. As our current formulation shows, the incoherence process, by no means, is restricted to large chaotic environments, but in fact is an intrinsic property of the open system dynamics. Hence, the Kraus decomposition derived here is valid for an arbitrary environment of an arbitrary dimension as long as the conditions nullifying the SEE are met.

It is noteworthy that our DFE condition $[\hat{B}_\mu, \hat{H}_B] = 0$ may seem a very strong requirement to suppress the formation of SEE. Nevertheless, physical situations exist in that this requirement is exactly satisfied. Examples include a spin spin–bath model with interactions modeled by an isotropic Ising-type coupling [22] and, as mentioned above, a quantum subsystem interacting with a chaotic bath of thermodynamics dimension [23]. One interesting question regarding our DFE condition is whether $[\hat{B}_\mu, \hat{H}_B] = 0$ is a necessary or only a sufficient condition for the emergence of absolute incoherence dynamics. Recent studies of decoherence show that the suppression of EID by chaotic baths maximizing intra-bath entanglement [23–28] and by non-chaotic baths with fast internal dynamics [29] is a generic effect, which is also independent of the type of system–environment coupling. This, in turn, suggests that $[\hat{B}_\mu, \hat{H}_B] = 0$ may just be a sufficient condition. To quantify the SEE, one can refer to the covariance function [31]

$$\mathcal{C}_\mu^n(t) = \mathrm{Tr}\{\hat{S}_\mu \hat{B}_\mu \hat{\rho}_n(t)\} - \mathrm{Tr}\{\hat{S}_\mu \hat{\rho}_n(t)\}\mathrm{Tr}\{\hat{B}_\mu \hat{\rho}_n(t)\}, \tag{18}$$

where $\hat{\rho}_n(t)$ is the time-evolved total density given by equation (11). In the absence of SEE, the covariance $\mathcal{C}_\mu^n(t) = 0$ and thus EID vanishes. In the light of recent studies [23–29], one can then expect that $\mathcal{C}_\mu^n(t) \to 0$ should lead to the absolute decoherence dynamics even though $[\hat{B}_\mu, \hat{H}_B] \neq 0$. By studying a number of examples in the following section, we will conclude that this is indeed the case.

3. Examples

Spin–bath models [32] have received considerable recent attention because of their relevance to quantum information processors. Here we study a spin spin–bath model to exemplify the incoherence process for a number of different situations including chaotic, regular and DFEs. We expect that any approximate condition nullifying the SEE should lead to the onset of the absolute incoherence dynamics. Since one of the objectives of our study is to make a clear distinction between the incoherence and EID processes, we have chosen our examples to test the validity of conditions supporting the absolute incoherence dynamics. To do so, we compare the predictions of the Kraus decomposition (15) to the exact numerical results obtained via the numerical solutions of the Liouville–von Neumann equation for our spin spin–bath model.

Our spin spin–bath model describes an open system dynamics of a qubit in an isolated many-qubit QC with static internal imperfections [29]. Residual static qubit–qubit interactions arising in a many-qubit QC core generate an unavoidable internal decoherence mechanism for ideal computational states of qubits [26–29]. Therefore, even though the external decoherence time due to a macroscopic environment is long enough, and thus the QC core can be considered as an isolated closed system, the qubits within such an isolated QC core experience their own nearby microscopic environment and are subject to internal decoherence dynamics [26–29].

Our isolated QC model is based on Josephson junction qubit architectures [33–35], which are promising information processor candidates due to their scalability and long external decoherence time [33–35]. Recently, we have investigated the effects of residual static

internal imperfection on the internal decoherence dynamics for a Josephson charge qubit QC [26–29]. Our results showed that even though decoherence by an external macroscopic environment is negligible, internal decoherence in an isolated QC core exists and may be an issue of concern. Moreover, we found that the alarming source of error was unitary due to environment-induced coherent shifts. Since incoherence dynamics originates from the coherent shifts, an environment of qubits based on a Josephson junction QC [33–35] is an ideal ground to study incoherence dynamics.

We present the mathematical details of our spin–spin bath model in section 3.1 and define the parameters used in our numerical calculations in section 3.2. We summarize our exact numerical approach in section 3.3 and give the explicit form of Kraus operators for our spin-bath model in section 3.4. We define open system quantifiers in section 3.5.

3.1. Model

Within very long external decoherence time for the Josephson charge qubit QC [35], we consider the QC core as a bipartite closed system represented by a total Hamiltonian of the form

$$\hat{H} = \hat{H}_S + \hat{S}\hat{B} + \hat{H}_B, \tag{19}$$

where the first term is the free system Hamiltonian of the central qubit

$$\hat{H}_S = -\tfrac{1}{2} B_0^z \hat{\sigma}_z^{(0)} - \tfrac{1}{2} B_0^x \hat{\sigma}_x^{(0)}, \tag{20}$$

and the second term is the coupling Hamiltonian mediating interactions between the central qubit and the nearby qubit environment:

$$\hat{S}\hat{B} = \hat{\sigma}_{x/z}^{(0)} \hat{\Sigma}_{x/z} \qquad \text{where} \quad \hat{\Sigma}_{x/z} = \sum_{i=1}^{N} \lambda_i \hat{\sigma}_{x/z}^{(i)}. \tag{21}$$

Here x/z means x or z. We consider xx-type (bit-flip errors) and zz-type (phase errors) interactions in separate calculations. We use the following effective self-interacting bath Hamiltonian to represent the nearby qubit environment of N qubits that the central qubit interacts with:

$$\hat{H}_B = -\frac{1}{2} \sum_{i=1}^{N} \left(B_i^z \hat{\sigma}_z^{(i)} + B_i^x \hat{\sigma}_x^{(i)} \right) + \sum_{i=1}^{N-1} \sum_{j=i+1}^{N} J_x^{i,j} \hat{\sigma}_x^{(i)} \hat{\sigma}_x^{(j)}. \tag{22}$$

Similar Hamiltonians are used in previous studies [26–29] of internal decoherence dynamics of qubits in isolated QCs with static internal imperfections and in investigations of effects of quantum chaos on quantum computation [30].

3.2. Numerics

Our numerical study is based on a charge-qubit QC proposal [35]. So, we scale the parameters of our Hamiltonian, accordingly, in units of $\epsilon = 200$ mK. The parameters of the central qubit are $B_0^{x/z} = 1\epsilon$, which are the experimentally relevant one-qubit control parameters. We set the value of system–bath coupling to $\lambda = 0.05\epsilon$, which corresponds to the two-qubit control parameter. We model one- and two-body intra-bath interactions, i.e. the parameters of the bath qubits, by following the previous studies [26–30]. Specifically, one-qubit parameters are sampled randomly and uniformly from the distributions $B_i^z \in \left[B_c^z - \delta_z/2, B_c^z + \delta_z/2\right]$ and $B_i^x \in \left[B_c^x - \delta_x/2, B_c^x + \delta_x/2\right]$, where B_c^x and B_c^z stand for the centers of the distributions and $\delta_{x/z}$ for the detuning parameters which we set to $\delta_{x/z} = 0.4 B_c^{x/z}$. We also sample residual

Table 1. A summary of numerical parameters used for different bath configurations.

Coupling	xx-type			zz-type		
Bath configuration	B_c^z	B_c^x	J_x	B_c^z	B_c^x	J_x
Case I	1	1	2	1	1	2
Case II	1	4	0	1	4	0
Case III(a)	0	1	0	1	0	0
Case III(b)	0	1	0.05	1	0	0.05

qubit–qubit interactions, i.e. system–bath and intra-bath interactions, randomly and uniformly from the distributions $\lambda_i \in [-\lambda,\ \lambda]$ and $J_x^{i,j} \in [-J_x,\ J_x]$, respectively. It should be noted that the chosen distributions for the bath parameters are rather narrow square boxes [26–30]. This is to reflect that qubits are relatively stable two-level systems. In an actual experimental situation, the type and magnitude of imperfections should be intrinsic to the experimental conditions and physical set-up. Therefore, the chosen distributions for our bath parameters should be considered as an idealization.

By three different choices of bath parameters we obtain three different cases, each of which supports the absolute incoherence dynamics. The numerical values of the bath parameters for three different cases are summarized in table 1. We use two different approaches to achieve the absolute incoherence dynamics for our examples. Our first approach is based on the facts that EID can be suppressed by chaotic baths [23–28] (case I) maximizing intra-bath entanglement [24] and by regular (non-chaotic) baths (case II) with fast internal dynamics [29]. Example studies by our first approach not only demonstrate the onset of absolute incoherence as a result of suppression of EID, but also display the notable distinction between the mechanisms of EID and incoherence processes. In our second approach, for case III, by manipulating certain intra-bath interactions we obtain exact, i.e. $[\hat{\Sigma}_{x/z}, \hat{H}_B] = 0$ (case III(a)) and approximate, i.e. $[\hat{\Sigma}_{x/z}, \hat{H}_B] \simeq 0$ (case III(b)) DFEs. To do so, we turn off certain intra-bath interactions which are not alike to the system–environment couplings. The approximate DFEs are obtained from the exact DFEs by setting the magnitude of the two-body intra-bath interaction strength to $J_x = 0.05\epsilon$ while keeping the other bath parameters fixed. The presence of the two-body intra-bath interactions spoils the symmetry conditions for DFEs. Consequently, the eigenstates of $\hat{H}_B$ are no longer the eigenstates of $\hat{\Sigma}_{x/z}$. However, since $J_x = 0.05\epsilon$ is a relatively weak coupling, still strong enough to induce EID, these eigenstates should be very similar.

For cases I and III, we set the inverse bath temperature to $\beta = 4\epsilon^{-1}$, which is the experimentally relevant temperature $\sim$50 mK for the charge-qubit QC proposal [33]. Exceptionally, for case II, a higher temperature $\beta = 1.2121\epsilon^{-1}$ is required for the emergence of decoherence. This is because the examples studied in case II are free of EID as well as decoherence by the incoherence process for $\beta = 4\epsilon^{-1}$. The strong $\hat{\sigma}_x$-type intra-bath interactions used to induce fast internal bath dynamics also caused a large energy gap between the ground and first excited states of the $\hat{H}_B$ spectrum [29]. As a result, the only ground state of $\hat{H}_B$ is populated for $\beta = 4\epsilon^{-1}$ for which no decoherence is observed [29].

3.3. Exact numerical approach

For the given parameters for each different case above, we calculated the exact eigenvalues E_n and eigenvectors $|n\rangle$ of the bath Hamiltonian by a Lanczos algorithm [36] for $N = 10$ bath qubits. This may seem a rather small bath size as compared to bath sizes used in the

simulations of external decoherence dynamics. However, for internal decoherence dynamics, the number of qubits that the central qubit interacts with is limited due to geometrical reasons unless very long-range residual qubit–qubit interactions exist in a QC core. In such cases, $N = 10$ would still be a small bath size. In this study, we simply ignore such long-range interactions for the sake of computational convenience.

For a product initial condition of the form $\hat{\rho}(0) = \hat{\rho}_S(0) \otimes \hat{\rho}_B(0)$, our initial subsystem state is

$$\hat{\rho}_S(0) = |\psi(0)\rangle\langle\psi(0)| \qquad \text{with} \quad |\psi(0)\rangle = (|0\rangle + |1\rangle)/\sqrt{2}, \tag{23}$$

and the initial thermal bath state is

$$\hat{\rho}_B(0) = \sum_{n=1}^{M} p_n |n\rangle\langle n| \qquad \text{with} \quad p_n = \exp\{-\beta E_n\} \Big/ \sum_{m=1}^{M} \exp\{-\beta E_m\}. \tag{24}$$

Since we are interested in the low-temperature regime, relevant to the charge-qubit QC [33, 35], $M = 20$ was a good approximation for all our examples. We obtained the exact quantum dynamics for the total density operator,

$$\hat{\rho}(t) = \sum_{n=1}^{M} p_n \hat{\rho}_n(t) \qquad \text{where} \quad \hat{\rho}_n(t) = |\Psi_n(t)\rangle\langle\Psi_n(t)|, \tag{25}$$

by numerically solving the Schrödinger equation $\mathrm{d}|\Psi_n(t)\rangle/\mathrm{d}t = -(\mathrm{i}/\hbar)\hat{H}|\Psi_n(t)\rangle$ with an eighth-order variable stepsize Runge–Kutta method [37] for each initial condition of the form $|\Psi_n(0)\rangle = |\psi(0)\rangle \otimes |n\rangle$, from which we obtained the reduced density operator $\hat{\rho}_S(t) = \mathrm{Tr}_B\{\hat{\rho}(t)\}$ by tracing over the environment degree of freedom.

3.4. Kraus approach

The Kraus operators for the Hamiltonian (19) take the form

$$\hat{\mathcal{K}}_n(t) = \sqrt{p_n} \exp\left\{\frac{\mathrm{i}}{2\hbar}\left(B_0^z \hat{\sigma}_z^{(0)} + B_0^x \hat{\sigma}_x^{(0)} - 2b_{x/z}^n \hat{\sigma}_{x/z}^{(0)}\right)t\right\}, \tag{26}$$

where $b_{x/z}^n = \langle n|\hat{\Sigma}_{x/z}|n\rangle$ are calculated by using the exact eigenstates $|n\rangle$ of the bath Hamiltonian for all different cases. The time evolution of reduced density matrix elements for the given temperature and initial condition is given by

$$\hat{\rho}_S(t) = \sum_{n=1}^{M} p_n \begin{pmatrix} \left|c_+^n(t)\right|^2 & c_+^n(t)\left[c_-^n(t)\right]^* \\ c_-^n(t)\left[c_+^n(t)\right]^* & \left|c_-^n(t)\right|^2 \end{pmatrix}, \tag{27}$$

where for the xx-type coupling:

$$c_\pm^n(t) = \frac{\sqrt{2}}{2}\left[\cos\left(\frac{a_x^n}{2\hbar}t\right) \pm \mathrm{i}\frac{\left(B_0^z \pm B_x^n\right)}{a_x^n}\sin\left(\frac{a_x^n}{2\hbar}t\right)\right], \tag{28}$$

$$a_x^n = \sqrt{B_0^{z\,2} + B_x^{n\,2}} \qquad \text{and} \qquad B_x^n = B_0^x - 2b_x^n, \tag{29}$$

and for the zz-type coupling:

$$c_\pm^n(t) = \frac{\sqrt{2}}{2}\left[\cos\left(\frac{a_z^n}{2\hbar}t\right) \pm \mathrm{i}\frac{\left(B_z^n \pm B_0^x\right)}{a_z^n}\sin\left(\frac{a_z^n}{2\hbar}t\right)\right], \tag{30}$$

$$a_z^n = \sqrt{B_z^{n\,2} + B_0^{x\,2}} \qquad \text{and} \qquad B_z^n = B_0^z - 2b_z^n. \tag{31}$$

3.5. Open system quantifiers

To characterize the open system dynamics, we employ two quantities: purity and fidelity. Purity is a good measure of non-unitary effects such as decoherence and dissipation. Fidelity on the other hand is sensitive to both non-unitary and unitary effects induced by an environment. In the presence of coherent shifting, purity or fidelity alone may not suffice for a complete characterization of the open system dynamics. Purity is invariant under unitary transformations and thus cannot detect environment-induced coherent shifts. Also, when unitary effects induced by an environment dominate non-unitary ones, it may not be possible to read the extent of decoherence off the fidelity. However, by tandem use of purity and fidelity, a comparison can be made and environment-induced unitary effects can be detected via the observation of uncorrelated time evolutions of purity and fidelity.

The purity is defined as the trace of the square of the subsystem's state,

$$\mathcal{P}(t) = \mathrm{Tr}_S\left\{\hat{\rho}_S^2(t)\right\}, \tag{32}$$

while the fidelity,

$$\mathcal{F}(t) = \mathrm{Tr}_S\left\{\hat{\rho}_S(t)\hat{\rho}_S^{\mathrm{free}}(t)\right\}, \tag{33}$$

where

$$\hat{\rho}_S^{\mathrm{free}}(t) = \exp\{-(\mathrm{i}/\hbar)\hat{H}_S t\}\hat{\rho}_S(0)\exp\{(\mathrm{i}/\hbar)\hat{H}_S t\} \tag{34}$$

is defined as an overlap between two states, the one of which undergoes the open system evolution and the other evolves unitarily under the free system Hamiltonian. The ideal values of purity and fidelity (i.e. in the absence of system–environment interactions) are unity for pure initial conditions. However, when the system–environment interactions are in effect, purity and fidelity deviate from their ideal value and take values less than unity.

Since our interest is in the incoherence part of decoherence dynamics, we also report our exact results for the canonical covariance [31] to determine to what extent the approximate conditions nullifying the SEE are actually satisfied. The non-vanishing values of the canonical covariance therefore indicate that the SEE exists and the open system dynamics also has contributions from EID. We calculate the covariance [31] for each populated pure state component of the canonical bath density for xx- and zz-type couplings,

$$\mathcal{C}_{x/z}^n(t) = \mathrm{Tr}\left\{\hat{\sigma}_{x/z}^{(0)}\hat{\Sigma}_{x/z}\hat{\rho}_n(t)\right\} - \mathrm{Tr}\left\{\hat{\sigma}_{x/z}^{(0)}\hat{\rho}_n(t)\right\}\mathrm{Tr}\{\hat{\Sigma}_{x/z}\hat{\rho}_n(t)\}, \tag{35}$$

from which we obtain the canonical covariance $\mathcal{C}(t) = \sum_{n=1}^{M} p_n\mathcal{C}_{x/z}^n(t)$. Hereafter, for simplicity, we refer to the canonical covariance as the covariance.

4. Results

In this section, we compare our exact numerical results to those of Kraus predictions for time evolutions of purity $\mathcal{P}(t)$ and fidelity $\mathcal{F}(t)$ to examine the validity of approximate conditions, i.e. $\mathcal{C}(t) \to 0$, supporting incoherence dynamics. We plot $\mathcal{P}(t)$ in figure 1 and $\mathcal{F}(t)$ in figure 2 for xx-type coupling, and $\mathcal{P}(t)$ in figure 3 and $\mathcal{F}(t)$ in figure 4 for zz-type coupling. Throughout the purity and fidelity figures we report our exact and Kraus decomposition results for case I (the chaotic environment) in subfigure (a), for case II (the regular environment) in subfigure (b) and for case III (approximate and exact DFEs) in subfigure (c). The time evolution of covariance $\mathcal{C}(t)$ is plotted in figure 5 for both xx- and zz-type couplings.

Both the purity and fidelity plots show very good agreements between the exact and Kraus results for both xx- and zz-type couplings. This indicates that the approximate conditions supporting incoherence dynamics can readily be achieved to a good extent. However, as

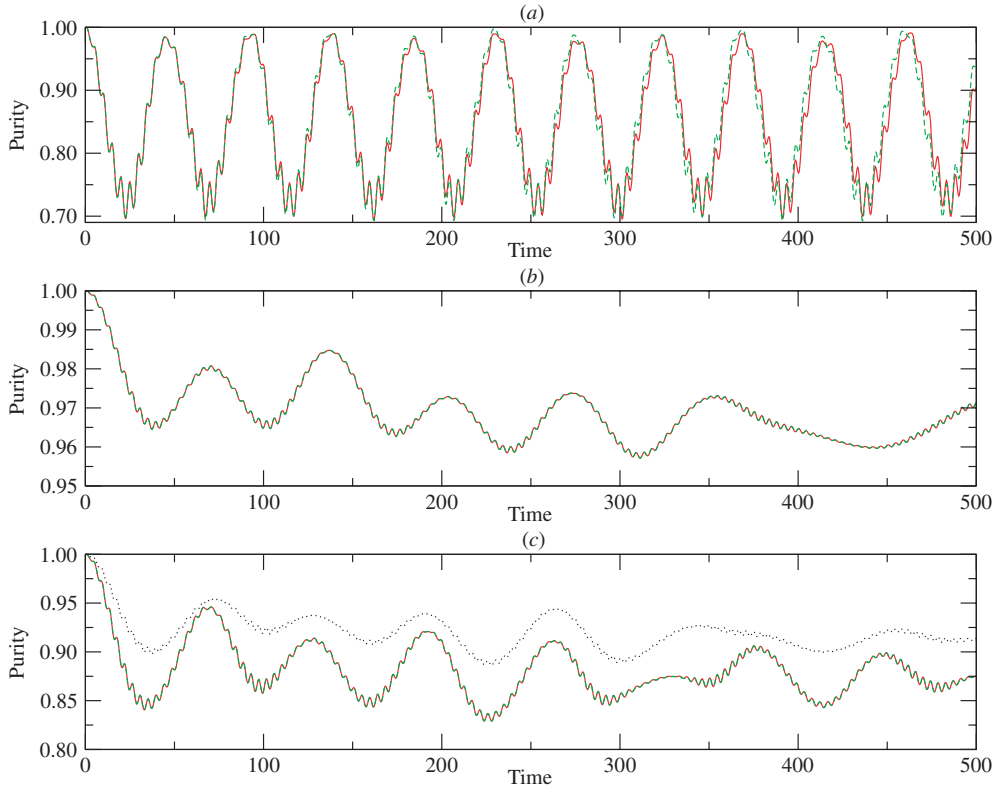

Figure 1. Time evolution of purity $\mathcal{P}(t)$ for exact (solid red) and Kraus decomposition (dashed green) results in the case of xx-type coupling plotted in (a) for case I, the chaotic environment; in (b) for case II, the regular environment and in (c) for case III, approximate and exact (dotted black) decoherence-free environments. Time is in units of $\hbar/\epsilon$ s.

indicated by the non-vanishing values of the covariance, EID is not completely suppressed for all cases. For the same type of system–bath coupling, the purity and fidelity plots show better agreements overall for case II than those observed for case I. For the different types of system–bath couplings, both the purity and fidelity plots display better agreements overall for xx-type coupling cases than those for the zz-type coupling.

In the case of the xx-type coupling, for case I, we see a very good agreement between the purity plots for a short timescale $t < 75\hbar/\epsilon$, but for a long timescale $t < 75\hbar/\epsilon$, a disagreement gradually evolves with time. The agreement between the fidelity plots is much better, and small discrepancies only appear after $t < 200\hbar/\epsilon$. For cases II and III, both the purity and fidelity plots show excellent agreements and the exact and Kraus results almost exactly overlap at all times. The better agreements observed for cases II and III as compared to case I can also be monitored from the covariance plots in figure 5(a).

In the case of the zz-type coupling, the purity plots for cases I and II display relatively large discrepancies as compared to the xx-type coupling cases. While the discrepancies for case I become more noticeable especially at long times, they do not worsen in time for case II. The overall agreement seems slightly better for case II than for case I. The fidelity plots also show noticeable discrepancies for both cases I and II for long dynamics. However, for short-time dynamics $t < 150\hbar/\epsilon$, the agreements are good. For case III, the purity plots

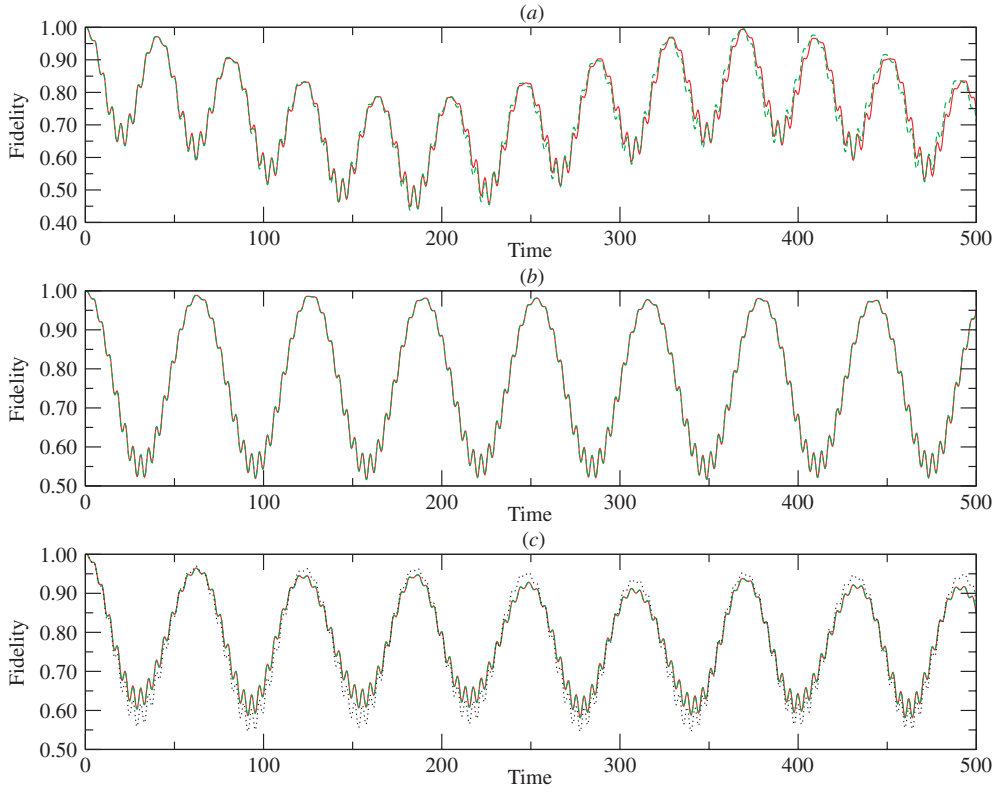

Figure 2. Time evolution of fidelity $\mathcal{F}(t)$ for exact (solid red) and Kraus decomposition (dashed green) results in the case of xx-type coupling plotted in (a) for case I, chaotic environment; in (b) for case II, regular environment and in (c) for case III, approximate and exact (dotted black) decoherence-free environments. Time is in units of $\hbar/\epsilon$ s.

show the largest discrepancies thus far and the agreement is only qualitative. Nevertheless, the fidelity plots are in very good agreement. The covariance plots display larger magnitude oscillations for the zz-type coupling which are indicators of disagreements between the exact and Kraus results due to EID. However, these disagreements are acceptable and overall the Kraus results are in very good agreement with the exact results.

We repeated our exact calculations a number of times for different realizations of the random parameters of $\hat{H}_B$ and compared our exact results to those of the Kraus decomposition. We always obtained qualitatively good agreements between the Kraus and exact results. Hence, the suppression of EID for cases I and II is quite generic effect, for at least the low-temperature regime. However, we did not observe the same degree of accuracy reported here in all our calculations. Especially for case I, we encountered some discrepancies between the Kraus and exact results for certain realizations of the random parameters of $\hat{H}_B$, which indicates that not all chaotic eigenstates, populated for the given bath temperature, are maximally entangled. However, in principle, a set of parameters should exist for which all populated bath states are maximally entangled and thus the absolute incoherence should be achievable. Our numerical study is limited to the low-temperature regime. It would be interesting to investigate decoherence dynamics for higher temperatures, where the number of populated bath states will be larger and thus EID as well as incoherence may show interesting behavior.

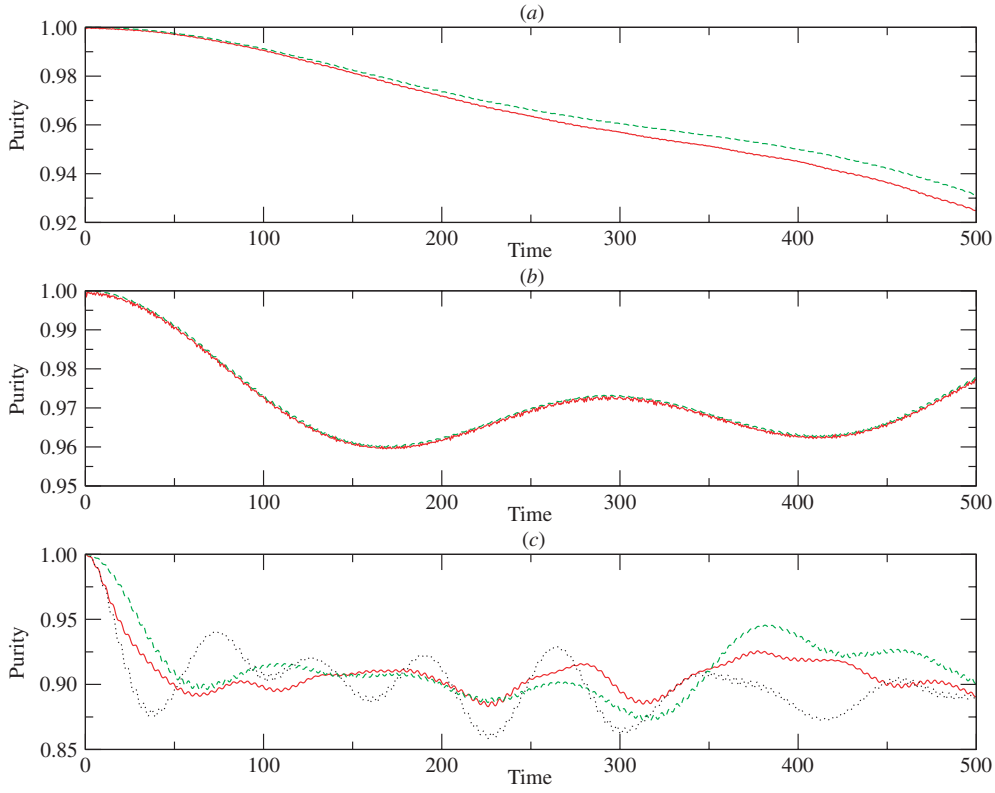

Figure 3. Time evolution of purity $\mathcal{P}(t)$ for exact (solid red) and Kraus decomposition (dashed green) results in the case of the zz-type coupling plotted in (a) for case I, the chaotic environment; in (b) for case II, the regular environment and in (c) for case III, approximate and exact (dotted black) decoherence-free environments. Time is in units of $\hbar/\epsilon$ s.

5. Discussions

This section is reserved for discussions of our results. Particularly, we discuss the origin of the good agreements observed between the exact and Kraus decomposition results, quasi-periodic behavior seen in the time evolutions of purity and fidelity, and approximate conditions supporting the absolute decoherence dynamics.

5.1. Exact versus Kraus decomposition results

To achieve the absolute incoherence dynamics, we followed two different approaches. In our first approach, in order to minimize the SEE, i.e. $\mathcal{C}(t) \to 0$, we used strong two-body intra-bath interactions to maximize intra-bath entanglement [24], and we used strong one-body intra-bath interactions to generate fast internal bath dynamics [29]. For case III, in our second approach, we obtained approximate DFEs, i.e., $[\hat{\Sigma}_{x/z}, \hat{H}_B] \simeq 0$ by turning off certain one-body intra-bath interactions which are not alike to system–bath couplings. Hence, the extent of the agreement between the exact and Kraus results for case I should primarily depend on whether the eigenstates of $\hat{H}_B$ are maximally entangled states, for case II it should depend on how effectively the fast internal dynamics prevents the formation of the SEE, whereas

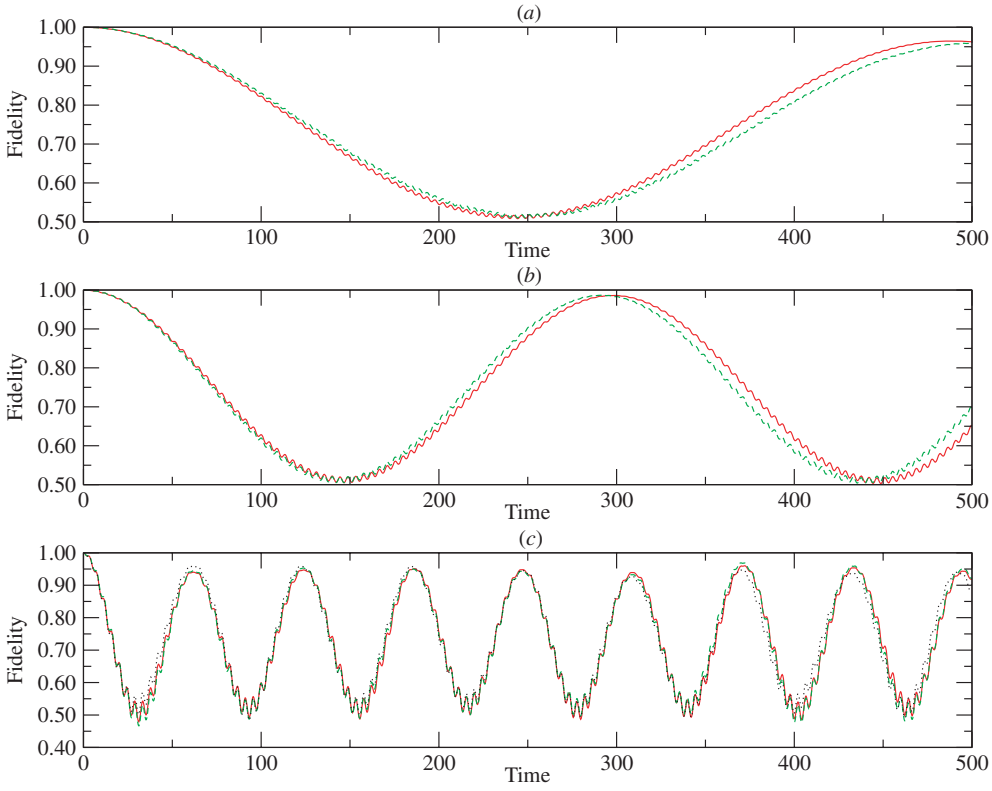

Figure 4. Time evolution of fidelity $\mathcal{F}(t)$ for exact (solid red) and Kraus decomposition (dashed green) results in the case of zz-type coupling plotted in (a) for case I, the chaotic environment; in (b) for case II, the regular environment and in (c) for case III, approximate and exact (dotted black) decoherence-free environments. Time is in units of $\hbar/\epsilon$ s.

for case III it should only depend on how close the eigenstates of $\hat{H}_B$ are to the eigenstates of $\hat{\Sigma}_{x/z}$.

We have obtained better agreements between the Kraus and exact results for xx-type coupling cases than for zz-type coupling cases. Recall that both one- and two-body intra-bath interactions we used were of $\hat{\sigma}_x$ type. Since the magnitude of these interactions was strong, as compared to system–environment couplings λ, the environment Hamiltonian $\hat{H}_B$ is dominated by $\hat{\sigma}_x$-type interactions for cases I and II. The alikeness of $\hat{\Sigma}_x$ and $\hat{H}_B$ suggests that the eigenstates of $\hat{H}_B$ are also the eigenstates of $\hat{\Sigma}_x$ or at least they must be very similar and thus $[\hat{\Sigma}_x, \hat{H}_B] \simeq 0$. Hence, the better agreements obtained for xx-type coupling cases can be explained as a result of extra contribution due to the similarity of the eigenstates of $\hat{\Sigma}_x$ to the eigenstates of $\hat{H}_B$. However, zz-type coupling cases do not have such an extra contribution. Since $\hat{\Sigma}_x$ and $\hat{\Sigma}_z$ are non-commuting operators, neither for case I nor for case II, the eigenstates of $\hat{\Sigma}_z$ should be similar to the eigenstates of $\hat{H}_B$. Therefore, the agreements between the exact and Kraus results in the case of zz-type coupling cases must be only because of the suppression of EID, i.e. $\mathcal{C}(t) \simeq 0$, via maximization of intra-bath entanglement for case I and fast internal bath dynamics for case II. Therefore, cases I and II for the zz-type coupling provide better representations of the effect of onset of absolute incoherence as a result of the suppression of EID.

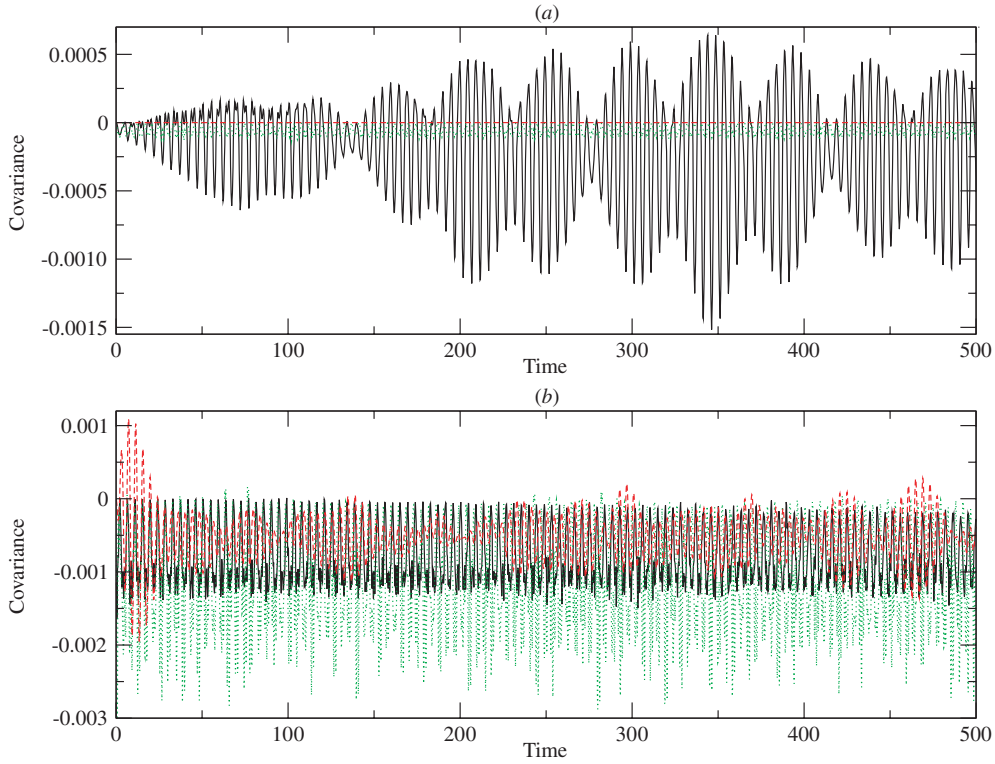

Figure 5. Time evolution of covariance $\mathcal{C}(t)$ plotted in (a) for xx-type coupling and in (b) for zz-type coupling. Case I: the chaotic environment (solid black), case II: the regular environment (dotted green) and case III: approximate decoherence-free environments (dashed red). Time is in units of $\hbar/\epsilon$ s.

As noted above, the Kraus decomposition of incoherence (15) is identical to the CKD derived in our previous studies [23]. While the CKD is only exact for the chaotic baths of thermodynamics dimensions, the prediction of the CKD against exact results for a chaotic bath of ten qubits showed excellent agreements [23]. The degree of accuracy obtained in these studies [23] was quite unusual, given that the thermodynamics limit is not attained for such a small bath of ten qubits and thus the off-diagonal matrix elements of the bath coupling operator, while can still be small, should not be vanishing. Our current results suggest that the accuracy of the Kraus decomposition for small chaotic baths, when the bath coupling operator and the bath Hamiltonians are non-commuting, can better be explained based on the saturation of intra-bath entanglement [24] rather than the vanishing off-diagonal matrix elements of the bath coupling operator. The example studied for case I and zz-type coupling represents such a case for which $[\hat{\Sigma}_z, \hat{H}_B] \neq 0$ but $\mathcal{C}(t) \simeq 0$.

The examples studied in case III test the DFE condition. To generate exact DFEs, we turned off one-body intra-bath interactions, i.e. $B_c^z = 0\epsilon$ for the xx-type coupling and $B_c^x = 0\epsilon$ for the zz-type coupling and the residual two-body intra-bath interactions, i.e. $J_x = 0\epsilon$ for both types of couplings. For approximate DFEs, we kept the two-body intra-bath interaction strength at $J_x = 0.05\epsilon$ to see how the mixing effect that it may cause affects the agreements between the Kraus and exact results. The better agreements observed for the xx-type coupling are again due to the similarity between the xx-type coupling and the two-body intra-bath

interactions. The presence of relatively small magnitude of two-body intra-bath interactions did not deteriorate the agreements in the case of the xx-type coupling, as also seen in the covariance plot in figure 5(a), but caused quite large disagreements between the purity plots in the case of the zz-type coupling. These large disagreements are the signatures of EID, as also indicated by the covariance plot in figure 5(b). The mixing effect induced by two-body intra-bath interactions can also be monitored by a comparison between purity and fidelity plots for approximate and exact DFEs. These interactions, while relatively weak, result in large differences in the order of magnitude of purities, especially for xx-type coupling case, but their effects on the fidelities are relatively weak.

5.2. *Quasi-periodic behavior in dynamics of purity and fidelity*

The purity and fidelity plots display a quasi-periodic to periodic behavior in some instances. The purity plot for the chaotic bath as seen in figure 1(a) shows some recurrences, whereas the purity plots for regular baths as seen in figures 1(b) and (c) do not. Moreover, the fidelity plots show some sort of periodicity in almost all cases, and neither the magnitude nor the dynamical behavior of fidelities does correlate with those of purities. The quasi-periodicity in purity emerges as a result of small number of populated bath states for the given low bath temperature. The magnitude of decoherence induced by incoherence dynamics grows with bath temperature: higher the bath temperature,–and thus the number of populated bath states—stronger the magnitude of decoherence in the system. Hence, the quasi-periodic behavior of purity completely disappears at higher temperatures with increasing number of populated bath states.

The quasi-periodicity of fidelities also arises due to the low bath temperature where the time evolutions of purity and fidelity do not correlate. While the quasi-periodicity of fidelity also disappears at high bath temperatures, where the dynamical behavior of purity and fidelity should correlate better, the fidelity dynamics also displays completely periodic behavior at absolute zero temperature, where decoherence vanishes. The periodicity in fidelity dynamics appears due to the fact that unitary effects induced by an environment dominate those of non-unitary ones at temperatures close to absolute zero. Since the purity is invariant under unitary transformation, it cannot capture the environment-induced unitary effects. The fidelity on the other hand is sensitive to both unitary and non-unitary effects. Hence, at very low temperatures, while the magnitude of purity stays very close to unity, the fidelity displays completely periodic behavior, and thus no correlation between purity and fidelity is observed.

The period of fidelity can readily be estimated at absolute zero, where incoherence dynamics is governed by a single Kraus operator $\hat{\mathcal{K}}_{n=1}(t)$, i.e. see equation (26). Here $n = 1$ stands for the ground state of the bath Hamiltonian. We obtained an analytic solution for the fidelity dynamics, which is very cumbersome, and is not reported here. We found that

$$\mathcal{F}(t) = \tfrac{1}{4}[3 + \cos 2(\omega_s - \omega_0)t] \tag{36}$$

is a perfect fit to the exact fidelity. Here $\omega_s = a_{n=1}/2h$ is the frequency of the shifted system Hamiltonian, where $a^{n=1}_{x/z}$ are given by equations (29) and (31) for xx- and zz-type coupling operators, respectively, and $\omega_0 = \left(B_0^{z\,2} + B_0^{x\,2}\right)^{1/2}/2h$ is the frequency of the coherent time evolution, see equation (20). Hence, the period of oscillatory fidelity dynamics is $\pi/(\omega_s - \omega_0)$ and is caused by the shift terms $b^{n=1}_{x/z}$, given in equations (29) and (31). At temperatures close to absolute zero, $\mathcal{F}(t)$ can also be approximated to a good degree by substituting $b^{n=1}_{x/z}$ with the canonical averages $\bar{B}_{x/z} = \mathrm{Tr}_B\{\hat{\Sigma}_{x/z}\hat{\rho}_S(0)\}$ in equations (29) and (31).

5.3. Approximate conditions supporting incoherence dynamics

In our numerical study, we aimed to make a clear distinction between incoherence and EID processes and test the validity of approximate conditions supporting absolute incoherence dynamics. In the formulation of incoherence dynamics, we exploited the symmetry condition $[\hat{B}_\mu, \hat{H}_B] = 0$ on bath coupling operators to suppress the EID $\mathcal{C}(t) = 0$. While this symmetry condition allowed us for a straightforward derivation of the Kraus decomposition (15), it appeared to be a rather strong assumption. Since recent studies of decoherence [23–29] indicate that the suppression of EID, i.e. $\mathcal{C}(t) \to 0$, does not require a particular symmetry condition on bath coupling operators, i.e. $[\hat{B}_\mu, \hat{H}_B] \neq 0$, it was of an interest to explore the performance of our Kraus decomposition for the approximate condition $[\hat{B}_\mu, \hat{H}_B] \neq 0$ but $\mathcal{C}(t) \to 0$.

We have chosen two particular examples (i.e. cases I and II for zz-type coupling $\hat{\Sigma}_z$) to test the validity of the Kraus decomposition for the approximate condition. For these two examples, while the environment dynamics was dominated by one– or two-body intra-bath interactions of $\hat{\sigma}_x$ type, i.e $[\hat{\Sigma}_z, \hat{H}_B] \neq 0$, we obtained very good agreements between the exact and Kraus results, along with $\mathcal{C}(t) \simeq 0$. These results suggest that $\mathcal{C}(t) \to 0$ leads to absolute incoherence dynamics even though $[\hat{B}_\mu, \hat{H}_B] \neq 0$. In such instances, equation (12) takes the approximate form

$$\hat{\rho}_n(t) \simeq \hat{U}_S^n(t)\hat{\rho}_S(0)\hat{U}_S^{n\dagger}(t) \otimes \hat{U}_B(t)|n\rangle\langle n|\hat{U}_B^\dagger(t), \tag{37}$$

which can be interpreted as follows: system–environment interactions act as perturbations on both system and environment degrees of freedoms. When an environment degree of freedom is stable against such perturbations, i.e. its dynamics, in a sense, evolves in a decoherence-free fashion as immune to the perturbations, the formation of non-local quantum correlations between system and environment degrees of freedom can be avoided. It follows then that the incoherence dynamics emerges as the only source of decoherence.

Our numerical results are limited to small spin baths designed for simulations of internal decoherence dynamics arising in an isolated QC core in the presence of residual qubit–qubit interactions. The external decoherence dynamics experienced by such an isolated QC core may display very different decoherence effects due to larger bath sizes, different and wider distributions of bath parameters and so forth. However, if the matter of interest is the agreement between exact and Kraus results, we expect our Kraus decomposition to be accurate as long as the conditions supporting absolute incoherence dynamics are met.

6. Summary

Decoherence is one of the biggest impediments to the development of quantum computing technologies. The system–environment entanglement is one of the well-known, though not the only, sources of decoherence. Even in the absence of system–environment entanglement, decoherence may not be avoided. The current study was concerned with an alternative mechanism of decoherence, i.e. the incoherence process, which originates from environment-induced coherent quantum fluctuations. We established a symmetry condition on system–environment interactions to separate the incoherence process from the entanglement-induced decoherence and formulated the exact equation of motion for a quantum subsystem undergoing the incoherence process. The equation of motion is of a Kraus decomposition form in which each Kraus operator in the decomposition is explicitly defined. We exemplified incoherence dynamics for a number of different situations including chaotic, regular and decoherence-free environments.

Acknowledgments

The author acknowledges the financial support provided by the Department of Chemistry, Simon Fraser University. Special thanks are due to Dr T Johansson and Dr P W Percival for carefully reading the manuscript.

References

[1] Nielsen M A and Chuang I L 2000 *Quantum Computation and Quantum Information* (Cambridge: Cambridge University Press)
[2] Bennett C H, Brassard G, Crépeau C, Jozsa R, Peres A and Wooters W K 1993 *Phys. Rev. Lett.* **70** 1895
[3] Ekert A K 1991 *Phys. Rev. Lett.* **67** 661
[4] Bennett C H and Wiesner S J 1992 *Phys. Rev. Lett.* **69** 2881
[5] Murao M, Jonathan D, Plenio M B and Vedral B 1999 *Phys. Rev.* A **59** 156
[6] Joos E, Zeh H D, Kiefer C, Giulini D, Kupsch J and Stamatescu I-O 2003 *Decoherence and the Appearance of a Classical World in Quantum Theory* (New York: Springer)
[7] Schlossauer M 2008 *Decoherence and the Quantum–to–Classical Transition* (Berlin: Springer)
[8] Breuer H-P and Petruccione F 2003 *The Theory of Open Quantum Systems* (New York: Oxford University Press)
[9] Gardiner C W and Zoller P 2004 *Quantum Noise* 3rd edn (Berlin: Springer)
[10] See, e.g., Anastopoulos C and Hu B L 2000 *Phys. Rev.* A **62** 033821
Haake F and Reibold R 1985 *Phys. Rev.* A **32** 2462
Caldeira A O and Leggett A J 1983 *Ann. Phys.* **149** 374
Caldeira A O and Leggett A J 1983 *Physica* A **121** 587
Feynman R P and Vernon F L Jr 1963 *Ann. Phys.* **24** 118
[11] Nakajima S 1958 *Prog. Theor. Phys.* **20** 948
Zwanzig R 1960 *J. Chem. Phys.* **33** 1338
Zwanzig R 1961 *Lectures in Theoretical Physics* vol 3 (New York: Interscience)
[12] Kraus K 1971 *Ann. Phys., NY* **64** 311
Kraus K 1983 *States, Effects and Operations: Fundamental Notions of Quantum Theory* (Berlin: Springer)
[13] Lindblad G 1976 *Commun. Math. Phys.* **48** 119
Gorini V, Kossakowski A and Sudarshan E C G 1976 *J. Math. Phys.* **17** 821
Alicki R and Lendi K 1987 *Quantum Dynamical Semigroups and Applications* (Berlin: Springer)
[14] Redfield A G 1957 *IBM J. Res. Dev.* **1** 19
Redfield A G 1965 *Adv. Magn. Reson.* **1** 1
[15] Milburn G J 1991 *Phys. Rev.* A **44** 5401
Milburn G J 2006 *New J. Phys.* **8** 96
[16] Zanardi P and Rasetti M 1997 *Mod. Phys. Lett.* B **11** 1085
[17] Lidar D A and Whaley K B 2003 Decoherence-free subspaces and subsystems *Irreversible Quantum Dynamics (Lecture Notes in Physics* vol 622*)* ed F Benatti and R Floreanini (Berlin: Springer) p 83–120 (arXiv:quant-ph/0301032)
[18] Lidar D A, Bacon D and Whaley K B 1999 *Phys. Rev. Lett.* **82** 4556
[19] Zurek W H 1981 *Phys. Rev.* D **24** 1516
Zurek W H 1982 *Phys. Rev.* D **26** 1862
Zurek W H 2003 *Rev. Mod. Phys.* **75** 715
[20] See, e.g., Weinstein Y S *et al* 2004 *J. Chem. Phys.* **121** 6117
Henry M K *et al* 2007 *Quantum Inf. Process.* **6** 431
[21] See, e.g., Breuer H-P 2007 *Phys. Rev.* A **75** 022103
[22] See, e.g., Krovi H, Oreshkov O, Ryazanov M and Lidar D A 2007 *Phys. Rev.* A **76** 052117
[23] Çetinbaş M and Wilkie J 2008 *Phys. Lett.* A **372** 990
Çetinbaş M and Wilkie J 2008 *Phys. Lett.* A **372** 1194
[24] Dawson C M, Hines A P, McKenzie R H and Milburn G J 2005 *Phys. Rev.* A **71** 052321
[25] See, e.g., Olsen F F, Olaya-Castro A and Johnson N F 2007 *J. Phys.: Conf. Ser.* **84** 012006
Pineda C, Gorin T and Seligman T H 2007 *New J. Phys.* **9** 106
Yuan X Z, Goan H-S and Zhu K-D 2007 *New J. Phys.* **9** 219
Relano A, Dukelsky J and Molina R A 2007 *Phys. Rev.* E **76** 046223
Gorin T, Pineda C and Seligman T H 2007 *Phys. Rev. Lett.* **99** 240405

Jing J and Ma H-R 2007 *Chin. Phys.* **16** 1489
Rossini D, Calarco T, Giovannetti V, Montangero S and Fazio R 2007 *J. Phys. A: Math. Theor.* **40** 8033
Rossini D, Calarco T, Giovannetti V, Montangero S and Fazio R 2007 *Phys. Rev.* A **75** 032333
Gorin T, Prosen T, Seligman T H and Žnidarič M 2006 *Phys. Rep.* **435** 33
Olaya-Castro A, Lee C F and Johnson N F 2006 *Europhys. Lett.* **74** 208
Ma X S, Wang A M, Yang X D and You H 2005 *J. Phys. A: Math. Gen.* **38** 2761
Yuan X Z and Zhu K D 2005 *Europhys. Lett.* **69** 868
Yuan X Z, Zhu K D and Wu Z J 2005 *Eur. Phys. J.* D **33** 129
Lucamarini M, Paganelli S and Mancini S 2004 *Phys. Rev.* A **69** 062308
Alicki R 2004 *Open Syst. Inf. Dyn.* **11** 53
Žnidarič M and Prosen T 2003 *J. Phys. A: Math. Gen.* **36** 2463
Tessieri L and Wilkie J 2003 *J. Phys. A: Math. Gen.* **36** 12305
Paganelli P, de Pasquale F and Giampaolo S M 2002 *Phys. Rev.* A **66** 052317
Prosen T and Seligman T H 2002 *J. Phys. A: Math. Gen.* **35** 4707
[26] Çetinbaş M and Wilkie J 2007 *Phys. Lett.* A **370** 194
[27] Çetinbaş M and Wilkie J 2007 *Phys. Lett.* A **370** 207
[28] Çetinbaş M and Wilkie J 2008 *J. Phys. A: Math. Theor.* **41** 065302
[29] Çetinbaş M 2008 in preparation
[30] Georgeot B and Shepelyansky D L 2000 *Phys. Rev.* E **62** 3504
Georgeot B and Shepelyansky D L 2000 *Phys. Rev.* E **62** 6366
Georgeot B and Shepelyansky D L 1988 *Phys. Rev. Lett.* **81** 5129
Benenti G, Casati G and Shepelyansky D L 2001 *Eur. Phys. J.* D **17** 265
Montangero S, Benenti G and Fazio R 2003 *Phys. Rev. Lett.* **91** 187901
[31] Davis R I A, Delbourgo R and Jarvis P D 2000 *J. Phys. A: Math. Gen.* **33** 1895
[32] Prokof'ev N V and Stamp P C E 2000 *Rep. Prog. Phys.* **63** 669
[33] Makhlin Y, Schön G and Shnirman A 2001 *Rev. Mod. Phys.* **73** 357, and references therein
[34] Nakamura Y *et al* 1999 *Nature* **398** 786
Martinis J M, Nam S and Aumentado J 2002 *Phys. Rev. Lett.* **89** 117901
Vion D *et al* 2002 *Science* **296** 886
Yu Y *et al* 2002 *Science* **296** 889
Chiorescu I *et al* 2003 *Science* **299** 1869
Simmonds R W *et al* 2004 *Phys. Rev. Lett.* **93** 077003
[35] You J Q, Tsai J S and Nori F 2002 *Phys. Rev. Lett.* **89** 197902
[36] Lehoucq R B, Sorensen D C and Yang C 1998 *ARPACK Users' Guide: Solution of Large-Scale Eigenvalue Problems with Implicitly Restarted Arnoldi Methods* (Philadelphia: SIAM)
[37] Hairer E, Norsett S P and Wanner G 1993 *Solving Ordinary Differential Equations: I. Nonstiff Problems (Springer Series in Computational Mathematics* vol 8*)* 2nd edn (Berlin: Springer)